Steady and pulsating flow past a heated rectangular cylinder(s) in a channel

Saxena, Ashish; Ng, Eddie Yin Kwee

2017

Saxena, A., & Ng, E. Y. K. (2017). Steady and pulsating flow past a heated rectangular cylinder(s) in a channel. Journal of Thermophysics and Heat Transfer, 32(2), 401-413. doi:10.2514/1.T5265

https://hdl.handle.net/10356/104714

https://doi.org/10.2514/1.T5265

Steady and Pulsating Flow past a Heated Rectangular Cylinder(s) in a Channel

Ashish Saxena[1] and Ng Yin Kwee, Eddie[2*]
[1,2]*School of Mechanical and Aerospace Engineering, Nanyang Technological University*

50 Nanyang Ave, Block N3, Singapore – 639798

**Email: MYKNG@ntu.edu.sg; Phone: (+65)6790 4455*

In the present study, the effect of laminar steady (Re=100, Pr=0.74) and pulsating flow (4 Hz and amplitude 0.4) is numerically studied over a centrally located heated rectangular cylinder of varying aspect ratio (W/H=1 to 8) in a confined channel using finite volume method. To study the influence of channel walls at a fix distance, eccentric placement of the highest aspect ratio cylinder(s) with two gap ratios (B/H) of 5 and 0.5 is done. Isotherms and streamlines of the flow are presented along with lift and drag coefficients. Further, FFT spectral analysis is performed to evaluate the vortex shedding frequency of the flow upon interaction with the cylinder(s). For single cylinder at the center position in the channel, natural vortex shedding and *"lock-on"* shedding occurs for lower aspect ratio cylinder under steady and pulsating flow, respectively. An increase in aspect ratio has a suppressing effect on the vortex shedding with a substantial decrease in the heat transfer over the cylinder. Placing two cylinders (W/H=8) at a geometrically symmetrical eccentric location of B/H=5 shows an extra peak at half of the flow inlet frequency in FFT spectral curve that possibly confirms the *"lock-on"* shedding with increased heat transfer over the cylinder.

Keywords: Vortex shedding, lock-on phenomenon, aspect ratio, gap ratio, pulsatile flow, channel flow.

Nomenclature

x	Streamwise coordinate (m)
y	Transverse coordinate (m)
u	Velocity in streamwise direction (m/s)
v	Velocity in transverse direction (m/s)
p	Dynamic pressure (Pa)
t	Time (seconds)
a	Pulsating amplitude, dimensionless
H	Width of the cylinder (m)
W	Length of the Cylinder (m)
B	Gap height from the bottom channel wall (m)
C_D	Drag coefficient, dimensionless $\left(=\frac{2F_D}{\rho U_o^2 l_c}\right)$
$\overline{C_D}$	Time average drag coefficient $\left(=\frac{1}{\tau}\int_0^{\tau} C_D\, dt\right)$
C_L	Lift coefficient, dimensionless $\left(=\frac{2F_L}{\rho U_o^2 l_c}\right)$
F_D	Drag force (N)
F_L	Lift force (N)
U	Inlet velocity (m/s)
U_0	Time average inlet velocity (m/s)
l_c	Characteristic length (m)
C_P	Specific heat capacity of fluid (J/kg K)
f	Dimensional frequency (Hz)
f_p	Pulsating frequency (Hz)
f_s	Vortex shedding frequency (Hz)
f_{sn}	Natural vortex shedding frequency (Hz)
k	Thermal conductivity of fluid (W/m K)
P	Perimeter of cylinder $(=2(H+W))$ (m)

Re	Reynolds number $\left(=\frac{U_o l_C}{\eta}\right)$
St	Strouhal number $(=\frac{f l_C}{U_o})$
Pr	Prandtl number, $(=\frac{\eta}{\alpha})$
T	Temperature (K)
T_w	Local surface temperature (K)
T_{in}	Inlet fluid temperature (K)
$Nu_{x,t}$	Local Nusselt number $(=\frac{hx}{k})$
h	Local heat transfer coefficient $(=\frac{q_w}{T_w - T_{in}})$
q_w	Heat flux from heated surface (W/m^2)
$\overline{Nu_{CW}}$	Time and space average Nusselt number over the cylinder $\left(=\frac{1}{\tau P}\int_0^{\tau}\int_0^{P} Nu_{x,t}\, dxdt\right)$
N	Number of mesh division in x −direction
M	Number of mesh division in y −direction

Greek symbols

α	Thermal diffusivity of fluid (m^2/s)
ρ	Density of fluid (kg/m3)
τ	Vortex shedding period for steady velocity inlet and pulsating time period for pulsating velocity inlet (seconds)
η	Kinematic viscosity (m^2/s)
μ	Dynamic Viscosity (N s/m^2)

I. Introduction

Fluid flow with heat transfer over bluff body is of great interest to the researchers since many decades. Application of such problems in aerospace engineering, electronic cooling, piping in the sea bed, flow obstruction by instrumentation and probes in chemical industries [1] etc. make it quite generic and attract many fundamental researches in the field [2,3]. Characteristic of vortex shedding at different Reynolds (Re) number [4], presence of local absolute instability in the existing wake [5], similarity relationships in oscillatory flows [6], concept of generation of parallel vortex shedding [7], sensitivity of critical Re number to the mode of primary vortex shedding[8], etc. are some of the important fundamental studies in the field. Given the wide applicability of flow across a cylindrical object, circular cylinder is the most studied geometry in the past [9–12].

Using finite volume method, Bijjam and Dhiman [13] studied the confined non-Newtonian flow over a circular cylinder. The authors have examined shear thinning and shear thickening behavior of the flow with vortex shedding for the Re range of 50-150. The authors have found out that shear thinning led to lower drag coefficient value as compared to Newtonian flow, while this behavior was found to be opposite for the case of shear thickening. The authors have also concluded that for a fixed power-law index, frequency of vortex shedding is proportional to the Re number. Owing to the practical application of forced convection heat transfer over multiple cylinders [14–16] in the field of heat exchanger, electrical equipment, mixing processes, etc.[17], Jue and Huang [18] studied the forced (Re=100 to 300) and mixed convection heat transfer characteristic over three cylinders oriented as right-angled isosceles triangle in a confined flow. The authors have varied the gap to diameter ratio in the range of 0.5-1.25 and found out that gap to diameter ratio of 0.75 yields a maximum heat transfer across all the flow conditions under study. Interestingly, given the relevance of geometrical shape in real time application, flow over a square cylinder attains a great attraction of researchers in the past [19,20].

Saha et al. [21] studied the low Re number (150-500) flow over a square cylinder in 3-dimension (3-D) to examine the different modes of vortex shedding. Studying the relationship between Strouhal (St) number, Reynolds number and drag coefficient, the authors have found out that 2-dimensional (2-D) shedding changes to 3-D in the range of Re = 150 to 175. Also, at Re = 250, secondary vortices change to small scale structures characterized by

discontinuity in St-Re relationship. Investigating the effect of working fluid on heat transfer, Dhiman et al. [22] examined the laminar flow (Re = 1 to 45) over a square cylinder for a range of Prandtl (Pr) number varying from 0.7 to 4,000. The authors have applied constant temperature and constant heat flux boundary conditions over the square cylinder and reported that average Nusselt (Nu) number increases with the increase in Re and/or Pr and is higher for the case of constant heat flux boundary condition. Studying the laminar flow for a further higher range of Re (50-160) and a short range of Pr (0.7 to 50), Sahu et al. [23,24] presented a similar trend in Nu variation against Re and/or Pr. Bayraktar et al. [25] studied high Re number (=20,000) flow over different cross-sectional cylinder geometry (viz. circular, square, diamond) placed near the wall for four different wall gap to cylinder width ratios using Spalart–Allmaras turbulence model. As the wall gap to cylinder width ratio increases, frequency of shedding also increases for all the geometries. Moreover, for a fixed ratio, circular cylinder gives the highest frequency of shedding. Introducing two square cylinder in a channel flow placed side by side in the orthogonal direction to the flow, Sau et al. [26] studied the development of vorticial structures through unsteady 3-D flow at fixed Re number 100 and varying gap ratios (gap/diameter) in the range of 0.2 to 2.1. The authors have concluded that flow wake behind the two square cylinders is highly 3-D depending on the gap ratio between the cylinders. The vortex shedding at high gap ratio remains locked in anti-phase synchronization. As the gap ratio decreases, the flow becomes more unstable and hence asymmetric with 3D dependent vorticial structures.

Changing the geometry from square to rectangular cylinder further suits many practical problems. Investigations performed in this direction avail an invaluable data in the field [27–29]. With the same motive, Norberg [30] performed an experimental study on rectangular cylinder with four different aspect ratios ranging from 1 to 3 placed in a cross flow ($R = 400\ to\ 30{,}000$). While varying the angle of incidence from 0^o to 90^o, the author has observed multiple wake frequencies at lower incidence angle and higher aspect ratios. Moreover, Strouhal number and drag coefficients were found to be constant for intermediate incidence angle. Next, work by Yang and Fu [31] and Srikanth et al. [32] examined the influence of oscillating rectangular cylinder in a cross flow to replicate the most realistic flow conditions. Lee et al. [33] studied the vortex shedding behind a rectangular cylinder placed near the wall for cylinder aspect ratio varying from 0.5 to 2 and wall gap to cylinder height ratio varying from 0.3 to 1.5 for a high Re number of 20,000. The authors have suggested ways to suppress the vortex shedding by attaching horizontal and vertical plates to the bottom surface of the cylinder that helps in shifting the maximum velocity point towards the wall and

hence, significantly suppresses the shedding. Similar results were presented by Kumaran and Vengadesan [34] for laminar flow (Re=450) across a square cylinder near the wall. For the lower gap ratios (< 0.6), a complete suppression of vortex shedding is observed.

From the literature survey, it has been pointed out that vortex shedding is an unavoidable phenomenon for the varied range of Re number. Also, aspect ratio and gap ratio (distance from the ground/channel wall) of the rectangular cylinder plays an important role in the on-setting or dampening of vortex shedding behind the cylinder. For a laminar steady flow regime, as the aspect ratio of the rectangular cylinder increases, the critical gap ratio above which vortex shedding induces also increases[33]. As the gap ratio reaches high enough that the wall has no influence on the flow over the cylinder, vortex shedding is supposed be only dependent on the aspect ratio of the cylinder and the flow inlet condition. Study on ceasing of the vortex shedding under steady laminar flow with the increase in aspect ratio is not done till date. Moreover, if the incoming flow across the cylinder with higher aspect ratio is itself pulsatile (in-line pulsation) in nature, then the wakes behind the cylinder could become unstable to induce vortex shedding. This in-line pulsating flow with certain range of frequency can control the vortex shedding, which is referred as *"lock-on"* phenomenon. This phenomenon is marked by an increase in lift and drag forces, which led to enhancement in the heat transfer over the cylinder. *"Lock-on"* phenomenon occurs when the vortex shedding takes place at a frequency equal to or half of the pulsation frequency for transverse or in-line pulsation, respectively [35,36].

Real-time scenarios like marine engineering, offshore exploration, power plants, etc. come across various engineering problems related to pulsatile flow and heat transfer across structures of circular and rectangular cross-sections. Anraka and Diller [37] experimentally studied high Reynolds number ($Re = 50{,}000$) pulsating flow with heat transfer across circular cylinder for a range of pulsating frequencies from as low as 0.67 Hz to 26 Hz with amplitude in the range of 4-25% of the mean flow. The authors have concluded that an increase of 30% in heat transfer near the separation can be achieved if both the pulsating and shedding frequency matches. Considering the turbulence intensity effect on the pulsating flow, Gundappa and Diller [38] presented similar results. Experimentally and numerically studying the low Reynolds number ($40 < Re < 810$) pulsating flow $\left(0.2 \leq f_p \leq 1.1\right)$ over circular cylinder, Iwai et al. [39] shown that a substantial increase in heat transfer happens during the low mean flow

velocity of pulsating flow. Experimental study on pulsatile flow ($Re = 350\ and\ 540$) across square cylinder of different blockage ratio at a fixed amplitude of 0.05 and varying frequency $(0 \leq f_p \leq 60)$ by Ho Ji et al. [40] revealed the occurrence of *"lock-on"* phenomenon. The authors have found that the occurrence of vortex shedding in the *"lock-on"* range of pulsating frequency results into enhancement of the convective heat transfer over the square cylinder. Yu et al. [41] reported a similar enhancement in heat transfer within *"lock-on"* regime through a numerical study on pulsatile flow ($Re = 100$) across square cylinder for a range of frequency $(0 \leq f_p \leq 20)$ and amplitude $(0.2 - 0.8)$. Hence, pulsatile inlet flow can augment the heat transfer over the cylinder within *"lock-on"* regime, but these studies are only limited to square cylinder. It is evident that the practical application of rectangular cylinders with aspect ratio more than 1 placed near or away from the ground/wall is of great practical relevance. Therefore, in the present study, a constant heat flux rectangular cylinder(s) with varying aspect ratio is placed at centric and eccentric positions in a confined laminar steady and pulsatile flow across a channel. Further, wake profile and its effect on the heat transfer over the cylinder is numerically studied. Evaluation of the cylinder aspect ratio at which vortex shedding ceases (placed at centric position in the channel) under steady flow condition is done. Thereafter, a corresponding effect of pulsatile flow on vortex shedding and heat transfer with increase in cylinder aspect ratio, placed at both centric and eccentric positions in the channel is studied.

II. Numerical Modeling and Simulations

A. Problem Description:

A rectangular cylinder of four different aspect ratios (W/H = 1, 3, 5.5 and 8) is placed at center position (gap ratio, B/H = 10 and H = 10 mm) of a two-dimensional confined channel flow ($Pr = 0.74$) as shown in Fig. 1a. Channel width is taken to be 20H. Upstream channel length from the front wall of the cylinder is 10H, while on the downstream side; channel length is taken to be 29H from the rear wall of the cylinder. For all the aspect ratio cylinders, steady and pulsatile inlet flow boundary conditions are examined at Re=100. Further, to study the wall effect on the thermohydraulics, the cylinder with highest W/H=8 is moved near the wall with two gap ratios (B/H) of 5 and 0.5, respectively, under pulsatile flow inlet boundary condition. For the given channel height, another cylinder of W/H=8 is placed at a geometrically symmetric position within the channel for the two B/H values (Fig. 1b), to study the influence of two cylinders along with the wall effect on the flow and heat transfer.

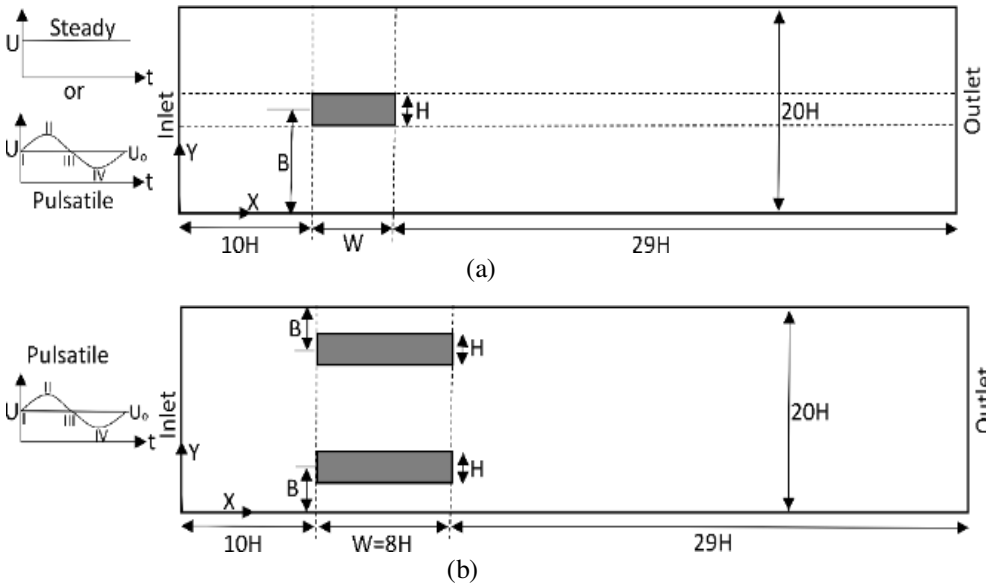

Fig. 1: Schematic diagram of physical domain (a) For centric cylinder placement (b) For eccentric cylinder(s) placement

To apply pulsatile flow inlet boundary condition, a sinusoidal pulsatile velocity profile is used with an amplitude (a) of 0.4 and pulsating frequency (f_p) of 4 Hz given by

$$U = U_o(1 + a.sin(2\pi f_p t) \quad \text{Eq. (1)}$$

It is observed in the work of Yu et al. [41] that a peak appears for the average coefficient of drag and enhancement in heat transfer (average Nu on the block) when the pulsating flow frequency of 4 Hz (for the given amplitude) is double of the natural shedding frequency over a square cylinder in a channel flow ($Re = 100$). Therefore, for the present study, analysis is done for the critical pulsating frequency (f_p) of 4 Hz. Average velocity (U_o) is calculated based on $Re = 100$ by taking height of the block as the characteristic length (l_c).

B. Mathematical Formulation:

The flow is assumed to be two dimensional, incompressible with constant thermal properties. To simulate the problem, flow and heat transfer governing transient Navier-Stokes and energy equations are solved, respectively, as expressed below in Cartesian coordinate system:

$$Continuity: \frac{\partial u}{\partial x} + \frac{\partial v}{\partial y} = 0 \quad \text{Eq. (2)}$$

$$Momentum: \frac{\partial u}{\partial t} + u\frac{\partial u}{\partial x} + v\frac{\partial u}{\partial x} = -\frac{1}{\rho}\frac{\partial p}{\partial x} + \eta\left(\frac{\partial^2 u}{\partial x^2} + \frac{\partial^2 u}{\partial y^2}\right) \quad \text{Eq. (3)}$$

$$and \ \ \frac{\partial v}{\partial t} + u\frac{\partial v}{\partial y} + v\frac{\partial v}{\partial y} = -\frac{1}{\rho}\frac{\partial p}{\partial y} + \eta\left(\frac{\partial^2 v}{\partial x^2} + \frac{\partial^2 v}{\partial y^2}\right) \quad \text{Eq. (4)}$$

$$energy: \frac{\partial T}{\partial t} + u\frac{\partial T}{\partial x} + v\frac{\partial T}{\partial y} = \alpha\left(\frac{\partial^2 T}{\partial x^2} + \frac{\partial^2 T}{\partial y^2}\right) \quad \text{Eq. (5)}$$

where, $\eta = \frac{\mu}{\rho}$ and $\alpha = \frac{k}{\rho C_P}$

C. Boundary Conditions:

Inlet: $u = U_o(1 + a.sin(2\pi ft), v = 0, T = 273K$

Outlet: Outflow boundary condition as $\frac{\partial \phi}{\partial t} + U_c\frac{\partial \phi}{\partial x} = 0$ [22–24,42], where the average streamwise velocity, $U_c = 1$ and ϕ is the dependent variable, $u, v \ or \ T$.

Top and bottom channel walls: $u = 0, v = 0, \ \frac{\partial T}{\partial y} = 0 \ (adiabatic)$

Cylinder walls: $u = 0, v = 0, \ \frac{\partial T}{\partial n} = -1 \ (constant \ heat \ flux)$

D. Numerical Procedure:

Governing equations are solved with the help of finite volume method using commercial CFD package FLUENT (version 17.1). Transient simulations are done on a two-dimensional grid using laminar solver. To save on the computing effort and being suitable for unsteady flows, PISO (Pressure Implicit with Splitting of Operator) scheme is used for pressure-velocity coupling. For interpolation of pressure values from the cell center values and spatial discretization of convection-diffusion equations, Body Force Weighted method and QUICK (Quadratic Upstream Interpolation for Convective Kinematics) scheme, respectively, are used. Unlike other spatial discretization schemes, QUICK scheme provides second order accurate solution for convection, while third order accurate solution

for diffusion equation. Energy equation is solved using upwind scheme discretized by finite difference method (second order accurate). For time discretization, fully implicit second order accurate scheme is used. Solution is converged with a residual value of 10^{-8} relative convergence criteria for continuity, $x-$ velocity and $y-$ velocity components, while a residual value of 10^{-10} for energy equation. All simulations are done on 6-compute node of an Intel(R) Xenon(R) E6-1660 v2 3.70 GH computer. A typical CPU time to complete 1 time-step is 67.91 seconds and 407.52 seconds for steady flow and pulsatile flow, respectively, across a square cylinder in a channel flow domain of 0.17 million grid size. Convergence is assumed to be reached once the periodic cycles of lift becomes consistent along with drag coefficient and the average Nusselt (Nu) number value over the cylinder becomes constant or indicates a consistent periodic variation with time.

E. Grid independent study and validation of Results:

Considering flow past a square cylinder (W=H) at the centric position in a channel with constant heat flux boundary condition over the cylinder block, four staggered grids defined by number of divisions in x - and y – directions (N x M): A(400x200), B(455x225), C(535x325) and D(595x385) are made using commercial ICEM software package. To study the grid independency, Coefficient of drag ($\overline{C_D}$), average Nusselt ($\overline{Nu_{CW}}$) number over the block and Strouhal (St) number are calculated as shown in Fig. 2. The percentage change in these values between mesh B and C is found to be 0.9%, 1%, and 1%, respectively, while between mesh C and D, the change is found to be 0.3%, 0.02%, and 0.8%, respectively. Therefore, for the computation, mesh C is used in the present study. Using staggered mesh C (Fig. 2a), the numerical method adopted is validated and results are compared with the previously published benchmark results as shown in Table 1. For different aspect ratio cylinder at centric and eccentric location, similar staggered mesh with number of elements in the range of 0.17 million to 0.28 million is used (refer Table 2 for more details).

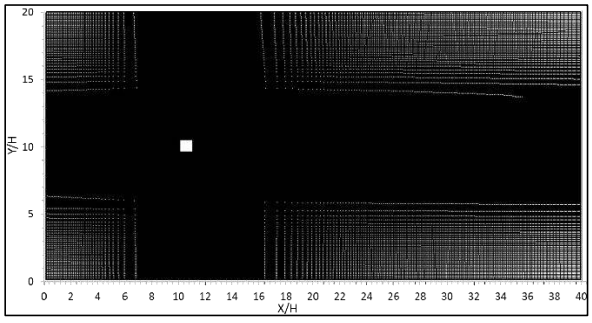

(a)

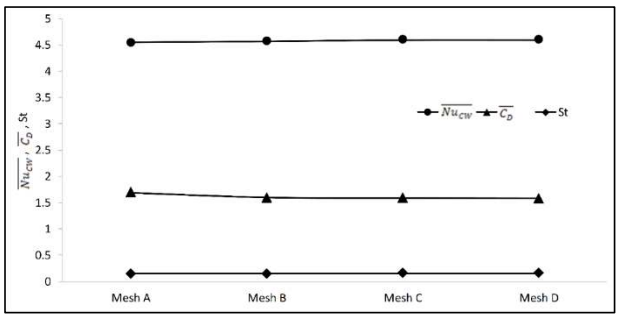

(b)

Fig. 2: (a) Mesh for square cylinder in the channel (b) Grid independence study plot

Table 1: Average Nusselt number, Strouhal number and average coefficient of drag for validation

Re=100, Pr=0.74	$\overline{Nu_{CW}}$	St	$\overline{C_D}$
Sahu et al. [23]	4.42	0.148	1.489
Yu et al. [41]	4.42	0.152	1.524
Sharma and Eswaran[42]	4.44	0.148	1.494
Present*	4.58	0.155	1.583

Table 2: Grid size for the various cases studied

Cases Studied	**Grid Size (N x M)**
W/H=1, B/H=10 Single Cylinder	535x325
W/H=3, B/H=10 Single Cylinder	585x325
W/H=5.5, B/H=10 Single Cylinder	648x325
W/H=8, B/H=10 Single Cylinder	710x325
W/H=8, B/H=0.5 Single Cylinder	710x325
W/H=8, B/H=0.5 Two Cylinders	710x380
W/H=8, B/H=5 Single Cylinders	710x325
W/H=8, B/H=5 Two Cylinders	710x400

III. Result and Discussion

Simulation results on placement of rectangular cylinder(s) with varying aspect ratio (W/H) across steady and pulsatile velocity inlet in a channel flow (Fig. 1) are presented in this section. Analysis on flow streamlines, isotherms, frequency of shedding, coefficient of lift (C_L), average coefficient of drag ($\overline{C_D}$), and heat transfer from the cylinder is done. For the pulsating flow inlet case, the isotherms and streamlines are plotted at the four equidistant instants (I-0^o, II-90^o, III-180^o, IV-270^o) of the sinusoidal velocity variation (Eq. 1). The spectral analysis (frequency domain) based Fast Fourier Transform (FFT) of the velocity data (in time domain) at the sampling point determines

the frequency of shedding. The relative coordinates of this sampling point are chosen to be at (H, 0.5H) from the rear top corner of the cylinder in the downstream.

A. Cylinder at Centric position:

Four cylinders with different aspect ratios (W/H=1, 3, 5.5 and 8) are placed at the centric position in a confined channel under steady and pulsatile flow inlet. For all the cases, the amplitude (A) of the FFT data is normalized with the amplitude ($A_{W/H=1}$) for the case of square cylinder (W/H=1) with steady velocity inlet. Further, variation of these parameters with W/H ratio is presented and discussed. Square cylinder with W/H=1 shows vortex shedding under steady flow at a natural shedding frequency ($f_{ns,W/H=1}$) of 2.27 Hz ($St = 0.155$) as shown in Fig. 4a. From Fig. 3, it is observed that the contours of isotherms and streamlines plotted at the four equal intervals of the shedding cycle are in good agreement with the work of Yu et al.[41] and Sharma and Eswaran[42]. There is a continuous formation and breaking of vortex from the top and bottom end of the rear wall of the cylinder, respectively. This sets in the cyclic vortex shedding in the downstream flow.

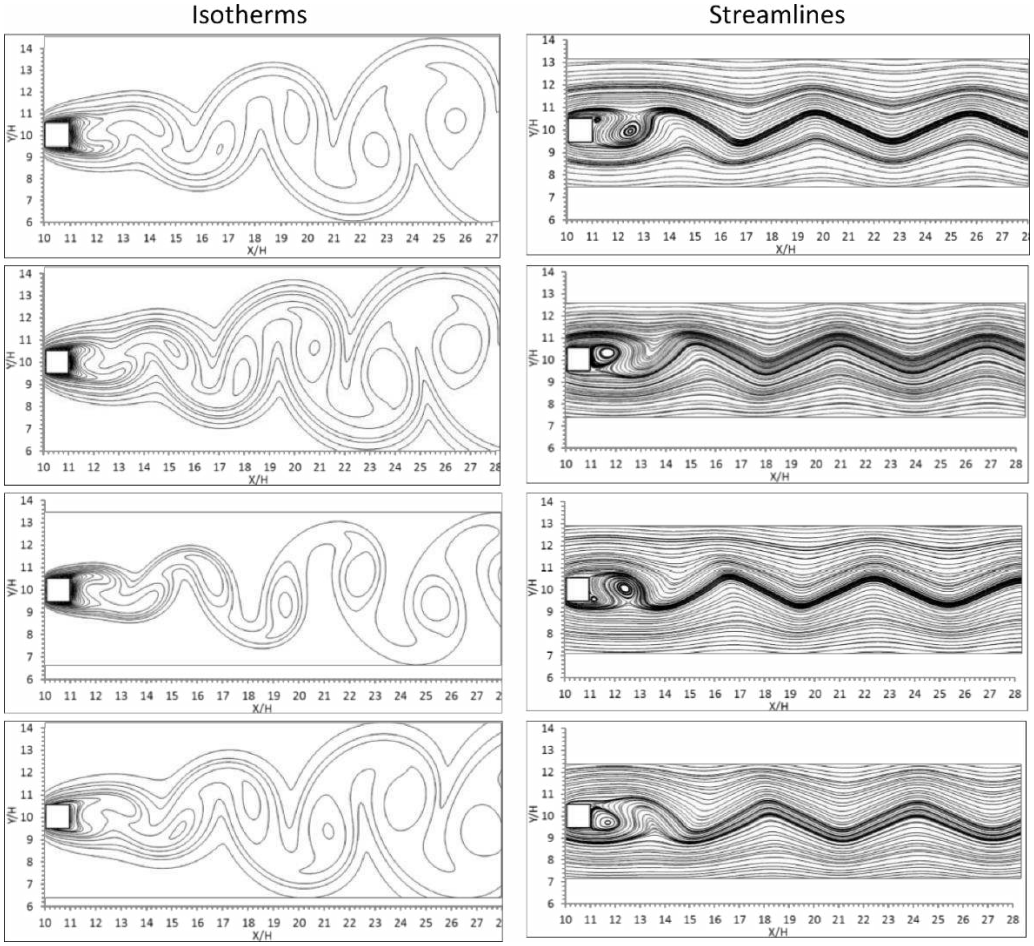

Fig. 3: Instantaneous isotherms and streamlines showing one cycle of vortex shedding at $f_{ns,W/H=1}$ of 2.27 Hz (from top to bottom: at C_L= 0, maximum, 0 and minimum) for cylinder with W/H=1 at steady velocity inlet (Re=100)

For the case of pulsating flow at the inlet, the intensity of vortex shedding is found to be increased as observed in the FFT plot (Fig. 4b) and the C_L plot (Fig. 5a). For both steady and pulsatile flows at the inlet, a growth in C_L oscillation is observed with each cycle of shedding; until the cyclic variation becomes consistent. However, for the latter case, with two peaks in each cycle of oscillation, the value of $C_L$is found to be almost 10 times greater than the former one. This is mainly because of the "*lock-on"* phenomenon as discussed in published literature [41 43–49]. The FFT plot in Fig. 4b shows an extra peak at a frequency (2 Hz) which is half of the flow pulsation frequency (4 Hz), confirms the occurrence of *"lock-on"* phenomenon in the present study.

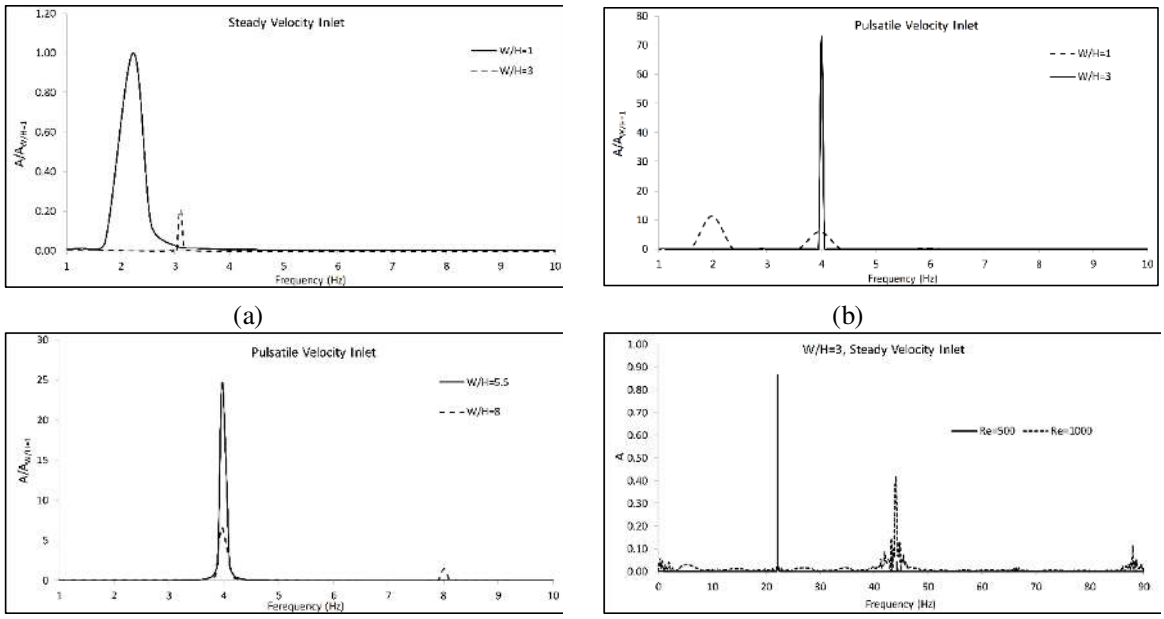

Fig. 4: FFT analysis of velocity at the sampling point (a) steady velocity inlet (Re=100) for W/H=1 and 3 (b) pulsatile velocity inlet (Re=100) for W/H=1 and 3 (c) pulsatile velocity inlet (Re=100) for W/H=5.5 and 8 (d) steady velocity inlet for W/H=3 at Re=500 and 1000

It is evident from the C_L plot in Fig. 4b that the time required for W/H=3 cylinder to set in the cyclic vortex shedding under steady inlet flow is delayed as compared to the case of W/H=1 cylinder. In addition, the cyclic trend is found to be squeezed in lesser time, which results into a higher shedding frequency ($f_{ns,W/H=3}$) of 3.11 from Fig. 4a. The trend in the isotherms and streamlines in Fig. 6 are found to be alike to the case of W/H=1 case, however, the shape and size of the vortex contours differ significantly. For the instant of maximum and minimum $C_L$value in the vortex shedding cycle, the size of the vortex formed at the top and bottom end of rear wall of the cylinder, respectively, is found to be 50% bigger for the case of W/H=3 (vortex size in x-direction = 1.5H) as compared to W/H=1 case (vortex size in x-direction = 1H). With the growth in vortex size due to increase in aspect ratio, isotherm contours for W/H=3 are found to be more elongated near the rear wall of cylinder, while in the downstream, the contours are less wavy as compared to the case of W/H=1.

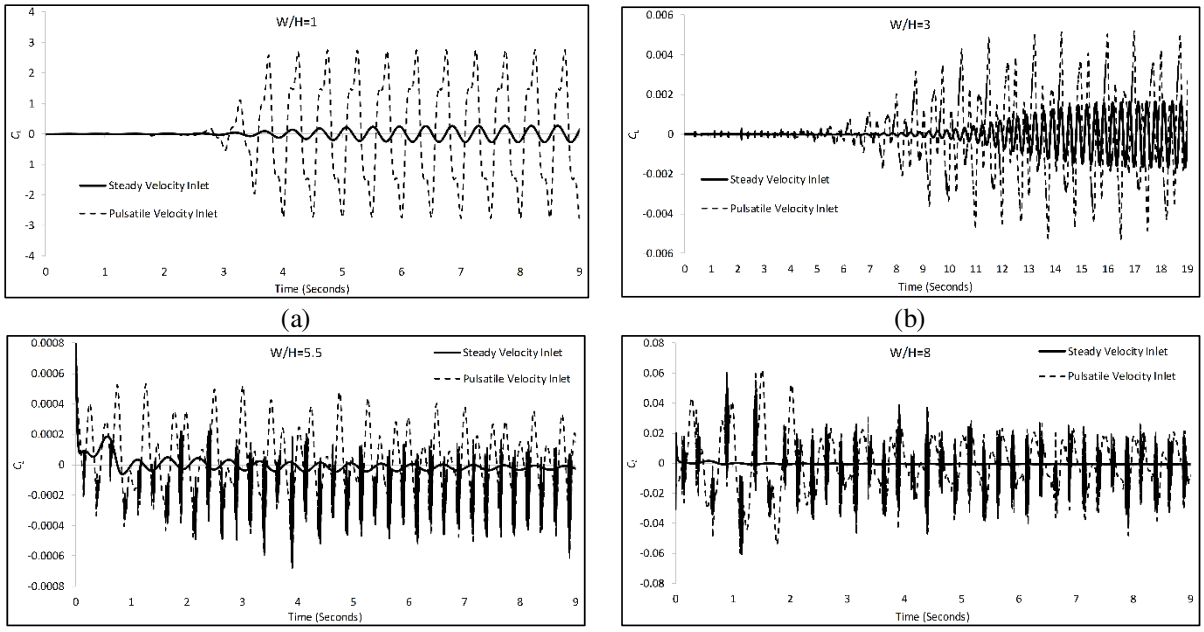

Fig. 5: C_L Oscillations for steady and pulsatile velocity inlet (a) W/H=1 (b) W/H=3 (c) W/H=5.5 (d) W/H=8

Given the lower FFT amplitude and $C_L$value for W/H=3 case as compared to W/H=1 case confirms the dampening effect due to increase in aspect ratio in the present study. To further understand the effect of steady inlet flow at higher Re on vortex shedding for W/H = 3 cylinder, simulations are done at higher Re as well. The FFT spectral analysis is performed over the velocity data at the same sampling point. Validation of these results is done against the experimental work of Atsushi Okajima[50], wherein wind tunnel tests were performed for the cylinder aspect ratio of 3 with a steady velocity inlet. A similar observation on the occurrence of a single peak at low Re of 100 and 500, and multiple peaks along with a dominant peak at high Re of 1000 is made in the present study as shown in Fig. 4 (a and d). Therefore, for the lower Re flow, even though dampening of vortex shedding happens with the increase in aspect ratio, the flow becomes chaotic with higher vortex strength as the Re value increases.

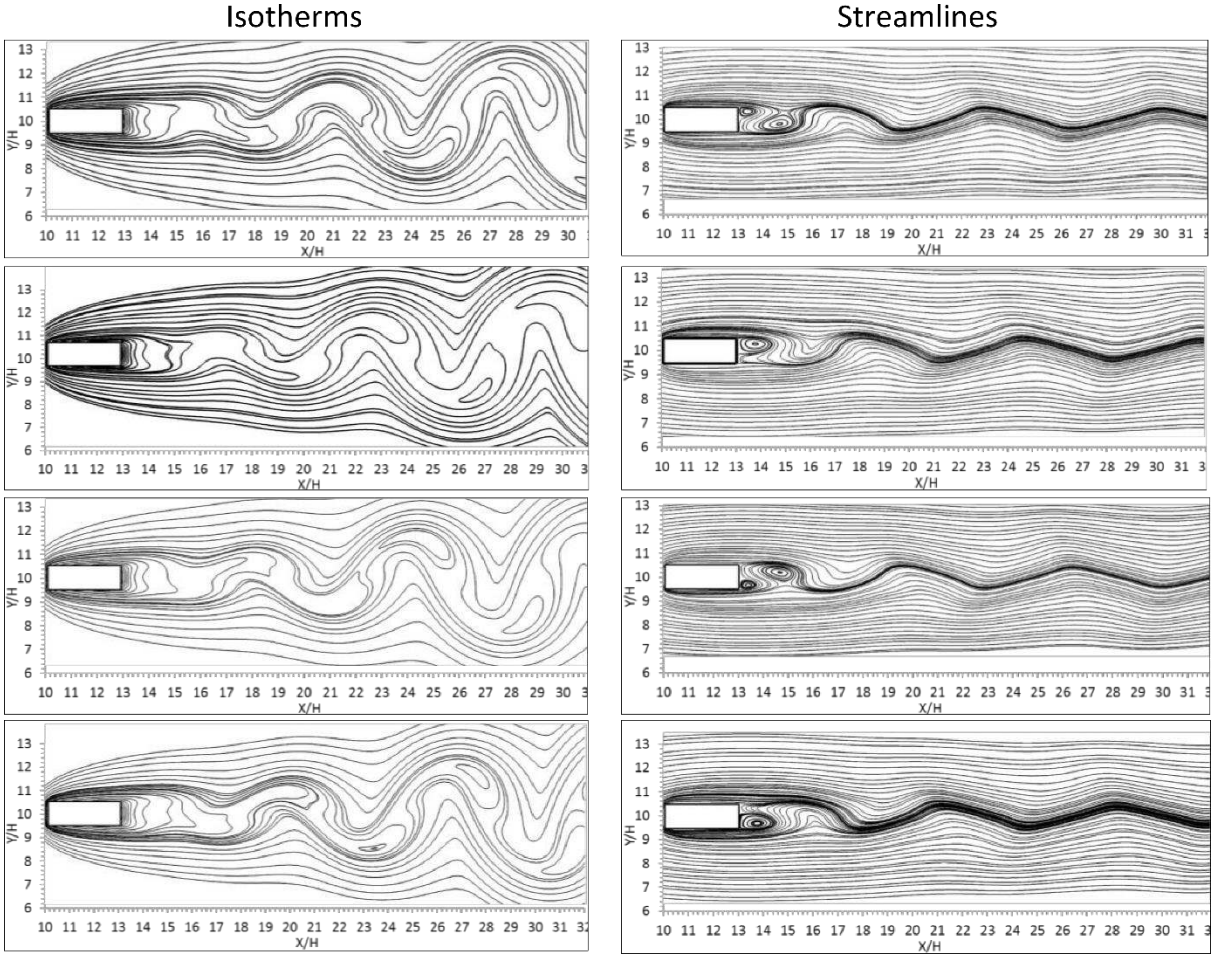

Fig. 6: Instantaneous isotherms and streamlines showing one cycle of vortex shedding at $f_{ns,W/H=3}$ of 3.11 Hz (from top to bottom: at C_L= 0, maximum, 0 and minimum) for cylinder with W/H=3 at steady velocity inlet (Re=100)

If for a certain application, Re number is limited to a lower value for a higher aspect ratio cylinder, a pulsatile flow inlet can be incorporated to negate the dampening effect of the cylinder. For a pulsatile inlet flow (as per Eq. 1) across W/H=3 cylinder, the intensity of C_L fluctuation due to shedding is found to be increased in comparison to steady inlet; however, the value of C_L for W/H=3 case is in the order of 10^{-3} as compared to order of 1 for the case of W/H=1. Moreover, the C_L shedding cyclic trend spreads along the time with several peaks within a single shedding cycle. Furthermore, from the FFT plot in Fig. 4b, a very small peak is noticed at around 3 Hz which is corresponding to the natural vortex shedding frequency, along with a dominant peak at 4 Hz which is corresponding to the inlet flow pulsating frequency. Given a situation where the inlet flow is pulsating at a frequency (f_p) of 6Hz which is almost double the natural shedding frequency ($f_{ns,W/H=3} = 3.11$) for W/H=3 cylinder, occurrence of *"lock-on"*

phenomenon can be expected. In the present study, to make a normalized comparison among different aspect ratios for the same inlet flow condition, only one pulsating frequency of 4 Hz is consistently used.

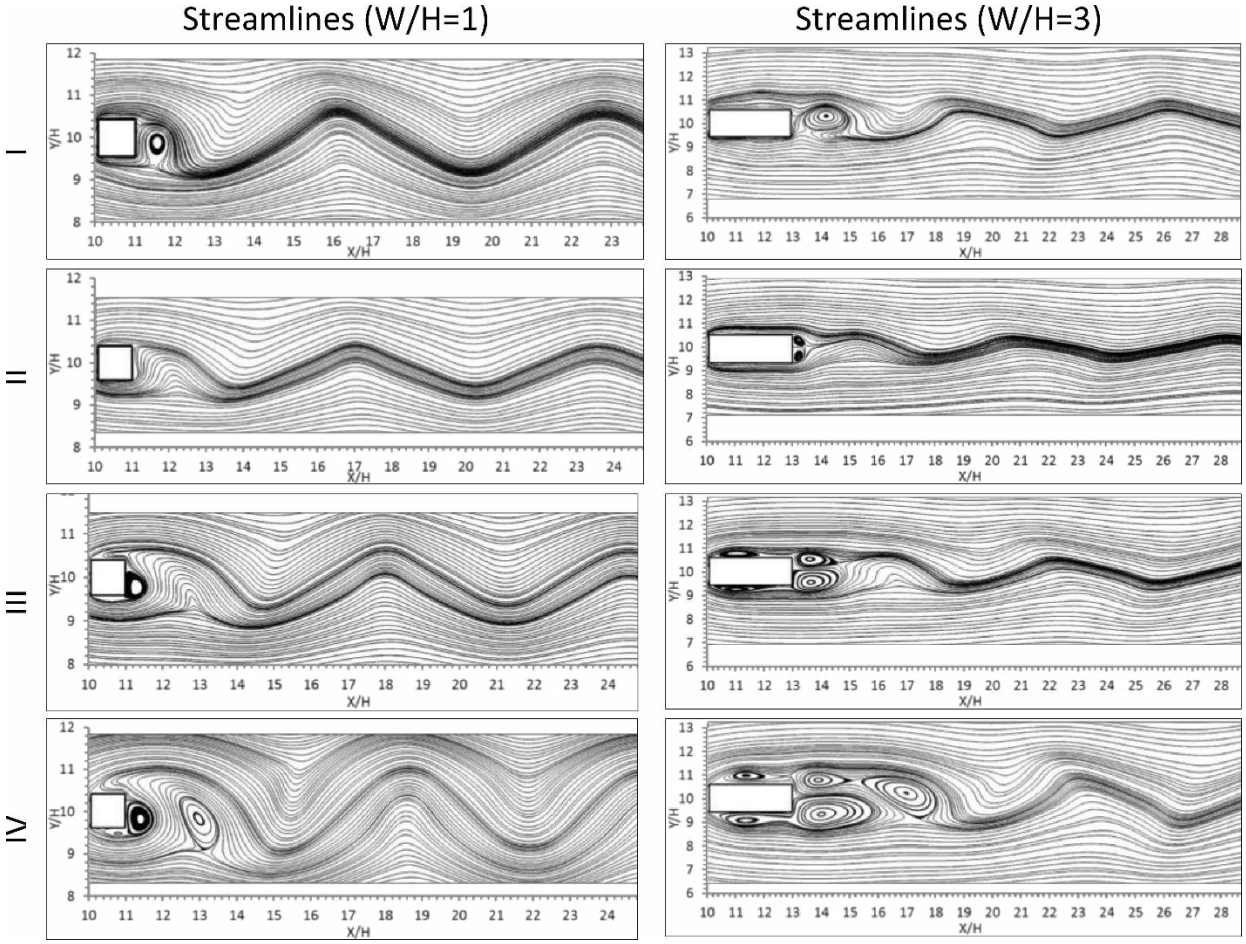

Fig. 7: Streamlines for cylinder with W/H=1 and 3 at four instants of pulsatile velocity inlet

Comparing the streamline contours between W/H=1 and 3 cases under pulsating flow inlet, there are significant differences observed as shown in Fig. 7. At instant (I) corresponding to the mean flow velocity, an elongated vortex (vortex size in x-direction = 1.5H) is formed along the streamwise direction for the case of W/H=3, which is 200% bigger in size than for the vortex (vortex size in x-direction = 0.5H) formed in W/H=1 case. For the maximum velocity instant (II), there is no vortex formed for W/H=1 case, while two small vortices are observed for W/H=3 case. Further (instant-III), the size of these two vortices (W/H=3 case) has unequally increased (maximum size of 1.5H in x-direction) with the formation of small vortices along the top and bottom walls of the cylinder (detachment of flow over the cylinder). At this instant (III), along with a small sized (0.5H) vortex near the rear wall of the

cylinder, a minute flow detachment over the horizontal walls of the cylinder is also observed for the case of W/H=1. For the minimum flow velocity instant (IV), enlarged multiple vortices are observed in the downstream (up to 5.5H from the rear wall of cylinder) and along the horizontal walls of the cylinder (W/H=3). Such downstream vortices are extended up to only 2.5H distance from the rear wall of the cylinder in the case of W/H=1. Therefore, it can be stated that increasing the length of the cylinder by 3 times led to a corresponding additional increase (add by a factor of 3H) in the distance up to which vortices are present at the minimum flow velocity instant.

As the aspect ratio (W/H) is further increased to 5.5 and 8, dampening of the shedding cycle is observed as shown in Fig. 5(c and d). Irrespective of the inlet flow conditions (steady or pulsatile), this decay in the amplitude of the C_L oscillation is noticed and the effect is found to be more dominant for W/H=8. Interestingly, the value of C_L variation has increased from the order of 10^{-4} to 10^{-2} as the aspect ratio increases from 5.5 to 8. For the steady flow inlet, the FFT spectral analysis revels no peak at all the frequencies, which confirms the absence of any periodic vortex shedding. Moreover, as the value of W/H increases from 5.5 to 8 under steady flow inlet condition, the isotherms and the streamlines (Fig. 8) are found to be similar and consistent over time. The vortex size for both the cases is found to be 2H in x-direction from the rear wall of the cylinder. Further, for the pulsating flow inlet, from the streamlines contours for instants III and IV in Fig. 9, a similar trend of multiple vortices formation (but more elongated) is observed as for the case of W/H=3. While vortices over the W/H=5.5 cylinder is found to be almost symmetrical along the horizontal axis of the cylinder, it is found to be asymmetrical with the increase in aspect ratio to W/H=8 at the minimum flow velocity instant (IV). Bigger vortices are formed along the bottom wall of the cylinder (W/H=8) as compared to the top, which is continued in the downstream length (length of bottom vortex is 2H more than top vortex in x-direction) with an extra vortex at the end. This extra downstream vortex is not present for the case of W/H=5.5. Therefore, flow over W/H=8 cylinder is supposed to be more unstable as compared to W/H=5.5 cylinder. This can be corroborated from the FFT spectrum analysis (Fig. 4c), where an additional peak at 8Hz is observed for W/H=8 cylinder along with a dominant peak at the flow pulsating frequency. For all the cylinders (W/H>1) studied under pulsating flow inlet, as the aspect ratio increases, the amplitude (from FFT) corresponding to the pulsating frequency of the flow decreases. This shows that after encountering the cylinder, the strength of inlet pulsation decreases with the increase in aspect ratio of the cylinder.

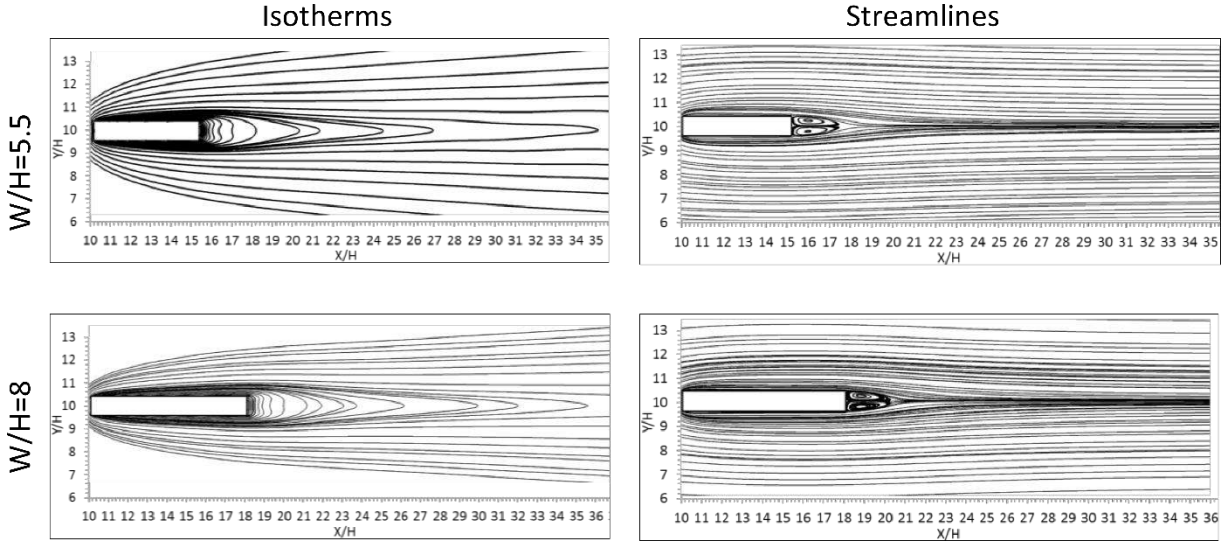

Fig. 8: Steady state streamlines (consistent over time with no shedding) for cylinder with W/H=5.5 and 8 at steady velocity inlet (Re=100)

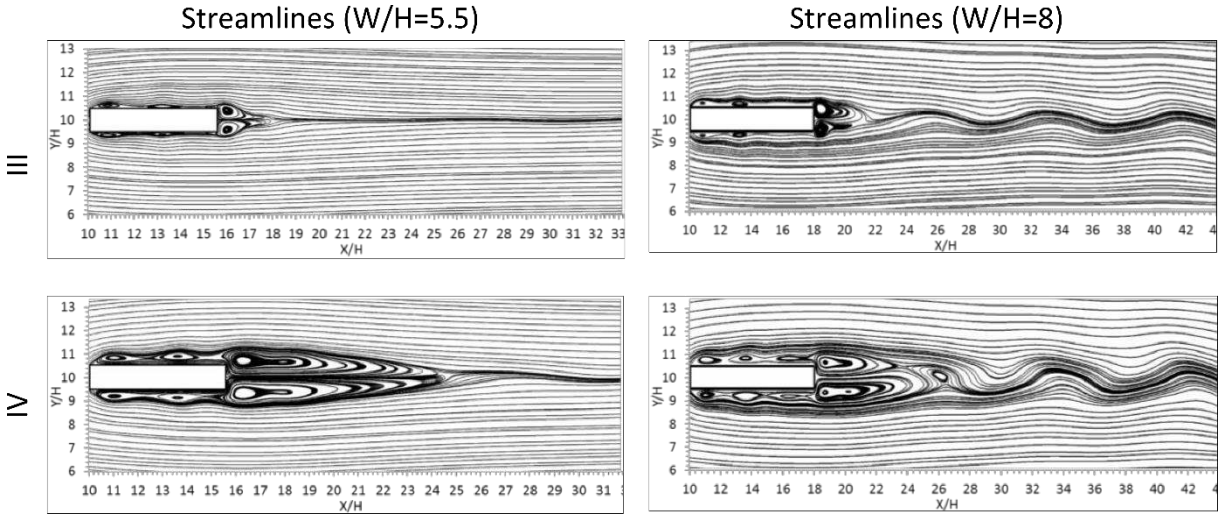

Fig. 9: Streamlines for cylinder with W/H=5.5 and 8 at III and IV instants of pulsatile velocity inlet

Time averaged coefficient of drag ($\overline{C_D}$) and Nusselt number over the cylinder ($\overline{Nu_{CW}}$) is calculated for all the cases and the results are plotted in Fig. 10. As the aspect ratio increases, the value of $\overline{C_D}$ first decreases and then increases under both steady and pulsatile flow inlet condition, except for W/H=1 case, where a lower value of $\overline{C_D}$ is observed under pulsatile flow inlet. Irrespective of the flow inlet condition (steady or pulsatile inlet), $\overline{Nu_{CW}}$ over the decreases with the increase in aspect ratio (W/H). For a given aspect ratio cylinder, pulsating flow inlet condition shows a higher $\overline{Nu_{CW}}$ as compared to steady flow inlet, which is in agreement with the increase in the magnitude of C_L oscillation under pulsatile flow inlet against steady flow inlet (Fig. 5). For W/H=1, enhancement in heat transfer

under pulsating flow inlet is found to be maximum with an enhancement of 1.36 times as compared to steady flow inlet. This enhancement in heat transfer is mainly because of the *"lock-on"* phenomenon which is marked by an increase in the magnitude of C_L oscillations and decrease in $\overline{C_D}$ value as compared to the steady flow inlet.

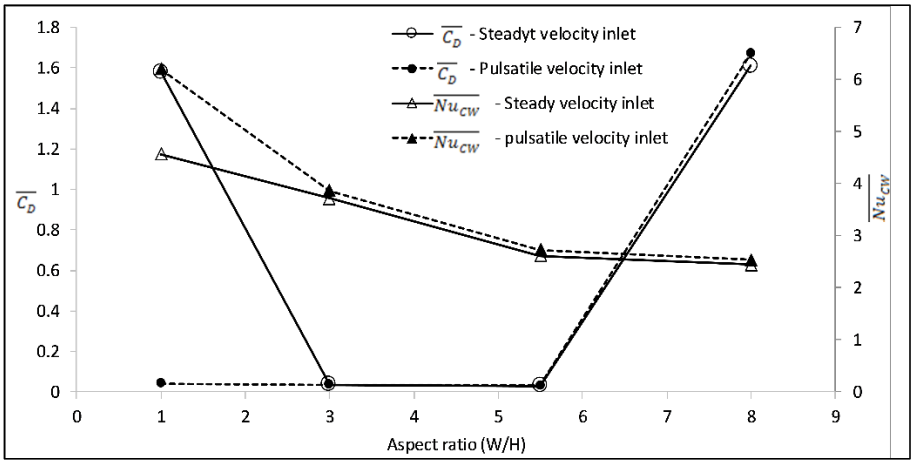

Fig. 10: $\overline{C_D}$ and $\overline{Nu_{CW}}$ variation with aspect ratio (W/H) under steady and pulsatile velocity inlet

Within pulsating flow inlet, as the aspect ratio increases from 1 to 3, 3 to 5.5 and 5.5 to 8, the corresponding decrement in the heat transfer is found to be 38%, 29% and 7%, respectively. For the case of W/H=3 and 5.5, even though the amplitude (from FFT spectral analysis in Fig. 4b) corresponding to the pulsating frequency of inlet flow is much higher than for the case of W/H=1, a huge decrement in heat transfer is because of the flow dampening effect with the increase in aspect ratio (lower C_L) and absence of any *"lock-on"* shedding. For W/H=8, under both steady or pulsatile flow inlet conditions, $\overline{C_D}$ is found to be the highest among all the aspect ratios studied, which is otherwise expected due to the size of the cylinder under same inlet flow condition. Under pulsatile flow inlet condition, the decrement in heat transfer for W/H=8 case is around 60% from W/H=1 case, whereas, even with a high $\overline{C_D}$ value, decrement in heat transfer is relatively small (only 7%) from W/H=5.5 case. This could be because of the relative increase in the magnitude of C_L oscillations due to relatively unstable asymmetrical flow across the W/H=8 cylinder (Fig. 9).

B. Cylinder(s) at Eccentric Position:

From the discussion in previous section (Section III A), it is evident that flow dampening is dominant for W/H=5.5 and 8 cylinders, which causes a decrement in the heat transfer under given steady flow inlet condition.

With the application of pulsating flow at the inlet, the corresponding heat transfer over the cylinder at a given aspect ratio can be increased, however, there is a decrement in heat transfer with the increase in aspect ratio. This decrement is found to be lowest when moving from W/H=5.5 to W/H=8 cylinder and expected to be consistent with any further increase in aspect ratio. Therefore, considering the highest aspect ratio cylinder (W/H=8) with other boundary conditions to be consistent, placing single and two cylinder(s) at two eccentric positions (B/H=5 and 0.5), study on the wall effect under pulsatile flow inlet is discussed in this section. Since instants (III) and (IV) of the pulsating cycle has shown significant changes in the flow, Fig. 11 shows the isotherms and streamlines at these instants for the eccentrically placed cylinder(s). Taking the advantage of symmetry (along the $x-$axis of the channel at $y = 10H$), flow over only one cylinder is shown in case of two cylinders. For this part of the analysis, the amplitude of the FFT data for the cases studied in this section is normalized with the amplitude of the FFT data for the pulsatile flow across a centric positioned (W/H=8) cylinder discussed in section III A.

As the W/H=8 cylinder moves from the centric position (B/H=10) to an eccentric position (B/H=5), at instants (III and IV) of the pulsatile cycle in Fig. 11a, similar asymmetrical vortices around the cylinder are observed (in Fig. 9), however, the vortices near the bottom wall of the cylinder (facing bottom wall of the channel) are either vanished or diminished in size. As a consequence of moving the cylinder near to the channel wall, the orientation of the uneven sized vortices generated behind the cylinder is reversed as compared to the case of centric position of the cylinder, and the length (in $x-$direction) from the rear wall of cylinder up to which these vortices are present is decreased by 9% and 7% for instant III and IV, respectively. At instant (IV) corresponding to minimum flow velocity, flow detachment due to formation of an elongated bubble, with several circulations within itself, is also observed at the channel wall (Fig. 11a). With the placement of second cylinder near the opposite wall with the same gap ratio (B/H=5), the size and shape of the vortices have further reduced. While the streamlines ending with sharp corners in the case of single eccentric cylinder, they are found to be smooth and rounded for the two eccentric cylinders case (Fig. 11b). Vortices along the rear wall of the cylinder are observed to be more circular, unlike elongated ones in the case of centric and single eccentric cylinder case. At instant III and IV, the second vortex along the rear wall of the cylinder and the third vortex in the downstream, respectively, have completely vanished. This has brought down the length (in $x-$direction) up to which vortices are present (from rear wall of cylinder) to

3H as compared to 8H in case of single eccentric cylinder at instant IV, with the persistent elongated bubble leading to detachment of flow at the channel wall.

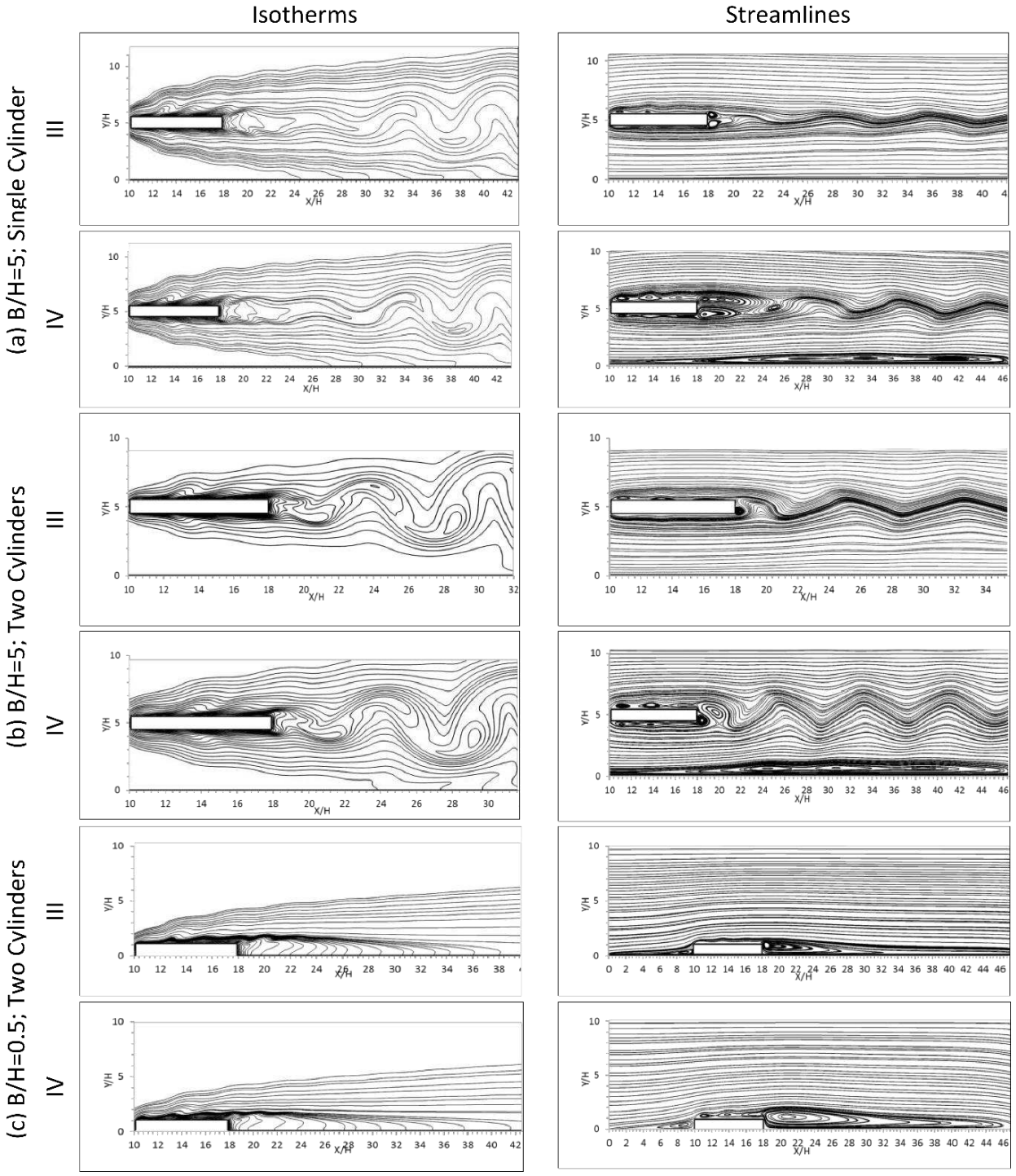

Fig. 11: Isotherms and streamlines for instant II and IV of pulsatile velocity inlet with W/H=8 cylinder(s) at eccentric locations (a) B/H=5, single cylinder (b) B/H=5, two cylinders (only one shown due to symmetry) (c) B/H=0.5, two cylinders (only one shown due to symmetry)

Placing the cylinder at the wall of the channel (B/H=0.5), flow streamlines and isotherms are found to be alike due to the wide channel width (20H) as compared to the height of the cylinders (H) and hence, only one of it is included in Fig. 11c. However, there are differences found in the other flow and heat transfer parameters that will be discussed later in this section. Moving the cylinder to the wall of the channel replicates the classic problem of low Re flows over a combination of forward and backward facing step geometry [51–53]. In the present study, the flow separates from the channel wall due to formation of a primary recirculation (clockwise direction) behind the cylinder for instant-I (mean flow velocity), which reattaches again at 8H from the rear wall of the cylinder in $x-$direction. The size of this primary recirculation in $y-$direction is well contained within the height of the cylinder (H). As the inlet flow reaches to maximum velocity (instant-II), there is no flow separation observed. A further decrease in the inlet velocity to mean flow velocity (instant-III) results into the formation of primary circulation on either side of the cylinder (in $x-$direction); along with the formation of secondary vortices over the horizontal wall of the cylinder (Fig. 11c). Moving to the minimum inlet velocity flow from instant (III) to (IV), the maximum size of primary vortex (in $y-$direction) near the front and rear wall of the cylinder has increased by 67% (from 0.6H to 1H) and 57% (from 1.4H to 2.2H), respectively; while the maximum size of secondary vortices (in $y-$direction) over the horizontal wall of cylinder has increased by 33% (from 0.6H to 0.8H).

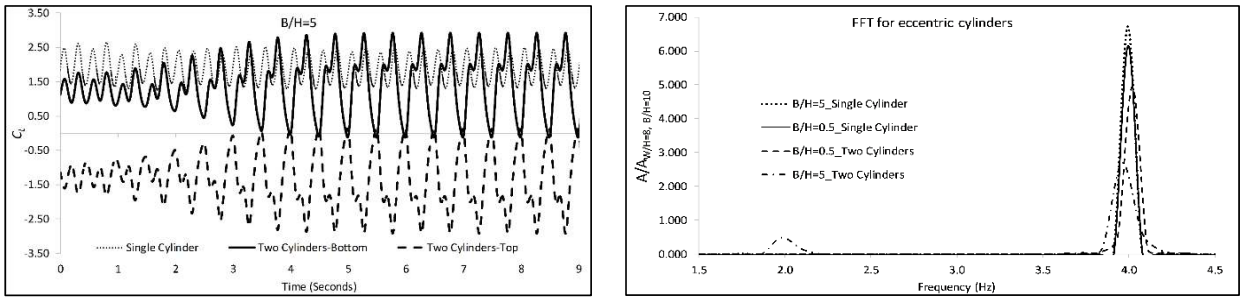

(a) (b)

Fig. 12: (a) C_L Oscillations for single and two cylinders (W/H=8) at B/H=5 (b) FFT of velocity at the sampling point for W/H=8 cylinder(s) at eccentric positions

For the case of single cylinder at the position B/H=5 near the bottom wall, C_L oscillations are observed to be less pronounced as compared to the case when another cylinder is placed at a geometrically symmetrical position. In case of two cylinders, while the $C_L$oscillation is positive for the bottom cylinder, it is found to be negative for the top cylinder, with the same magnitude (Fig. 12a). The negative value of $C_L$oscillation for the top cylinder is mainly

because of presence of the channel wall just above it. Further, with two cylinders, the amplitude of C_L oscillations grow with time before becoming consistent; while for the single cylinder case, it is consistent throughout with slight variations within a single cycle of oscillation. For both single and two cylinder(s) at B/H=0.5, C_L oscillations with same frequency but 50% less in magnitude for two cylinders case (C_L=±1.6) are observed. Through FFT spectral analysis, the effect of the position and the number of cylinders on the amplitude of inlet flow pulsation is determined. It can be observed from Fig. 12b that the pulsation amplitude for eccentric placement of the cylinder(s) is always higher than the centric placement. While single cylinder at B/H=5 location shows the maximum amplitude, introducing another cylinder at a geometrically symmetrical location (B/H=5) shows the minimum amplitude. Amplitude for the cylinder(s) at the walls (B/H=0.5) falls between the other two cases (Fig. 12b).

Table 3: Average Nusselt number and average coefficient of drag for eccentric placement of block

Case (W/H=8)	$\overline{C_D}$	$\overline{Nu_{CW}}$
B/H = 10	1.67	2.54
B/H = 5, Single Cylinder	1.78	2.59
B/H = 5, Two Cylinders	2.17	2.74
B/H = 0.5, Single Cylinder	0.018	2.26
B/H = 0.5, Two Cylinders	0.9	2.08

With the placement of two cylinders at B/H=5 and B/H=0.5, the frequency corresponding to the peak amplitude is found to be less (3.96 Hz) and more (4.02 Hz) than the inlet flow pulsating frequency (4 Hz), respectively. Moreover, only for two cylinders at B/H=5 case, an additional small peak is observed at a frequency of 1.98 Hz which is half of the dominant peak frequency (Fig. 12b). This possibly indicates the occurrence of natural shedding accompanied by *"lock-on"* phenomenon. It can be noted from Table 3 that the value of both $\overline{C_D}$ and $\overline{Nu_{CW}}$ have increased as the cylinder is shifted from centric to eccentric position (B/H=5). With the placement of the second cylinder at the geometrically similar eccentric position of B/H=5, these values (calculated over individual cylinder) are further increased, which is highest for all the cases examined under this section. This increase in $\overline{C_D}$ and $\overline{Nu_{CW}}$ can be corroborated from the fact that less vortices are formed behind the cylinder(s) at mean and minimum inlet flow velocity instants (III and IV) and a possible occurrence of *"lock-on"* phenomenon. On further moving the

cylinder(s) to the wall at B/H=0.5, a further decrement in the value of $\overline{C_D}$ and $\overline{Nu_{CW}}$ is noticed. There could be two reasons for this change: (i) Calculation is done only for the three walls of the cylinder due to merging of one of the horizontal walls of the cylinder with the channel wall (ii) During the decelerating phase of the inlet pulsating flow, multiple growing vortices are observed along the walls of the cylinder, which possibly negates the resultant drag force and reduces the effective heat transfer over the cylinder.

IV. Conclusions

In the present study, a finite volume based numerical approach is used to study the effect of cylinder aspect ratio (W/H) on the flow and heat transfer across a heated rectangular cylinder, placed at the centric position of a channel flow (Re=100) under steady and pulsatile velocity inlet, respectively. Four different aspect ratios are considered ranging from 1 to 8. Further, the effect of wall and placement of two cylinders (with the highest aspect ratio) on a geometrically symmetrical position along the channel width under pulsatile flow is also studied. For this case, two gap ratios are used, viz. B/H = 5 and 0.5. For all the cases, isotherms and streamlines of the flow are plotted along with the calculation of flow and heat transfer parameters, viz., coefficient of drag, coefficient of lift, and Nusselt number. Further, FFT spectral analysis of the velocity data at a sample point in the downstream is performed to determine the shedding frequency in various cases.

Under steady velocity inlet, placing the cylinder at the centric position in the channel shows an increase in the frequency of shedding from 2.27 Hz to 3.11 Hz as the aspect ratio increases from 1 to 3. This increase in shedding frequency is accompanied by a decrease in the magnitude of C_L oscillation and a substantial decrease in the heat transfer over the cylinder. Any further increase in the aspect ratio (W/H=5.5 and 8) led to a complete dampening of the vortex shedding (no peak in FFT analysis), which results into consistent streamline contours over time, followed by a low heat transfer over the cylinder. For the pulsatile velocity inlet, *"lock-on"* vortex shedding is observed for the lowest aspect ratio cylinder (W/H=1). As a result, the magnitude of C_L oscillation has further increased along with a corresponding enhancement in heat transfer by 1.36 times against steady flow inlet. This enhancement in heat transfer is maximum among all the aspect ratios studied. For W/H>1, the amplitude of pulsating frequency decreases with the increase in aspect ratio, which shows the dampening of pulsating flow due to increase in length of the

cylinder, followed by a decrease in heat transfer over the cylinder. However, for a given aspect ratio cylinder, heat transfer is always better than the steady flow inlet case.

For W/H=8, unlike the case of W/H=5.5 cylinder, an asymmetrical flow around the cylinder is observed, which induces an instability in the flow and shows an extra peak at double the value of flow pulsating frequency in the FFT spectrum. During the deceleration instants (III and IV) of the pulsating flow, the formation of multiple vortices in the downstream and around the cylinder is accounted for the decrease in heat transfer with the increases in size of the cylinder (W/H). Exhibiting the most dampening effect over the flow with relatively small change in heat transfer from the case of W/H=5.5 cylinder, cylinder with W/H=8 is chosen to be placed at eccentric positions (B/H=0.5 and 5) in the channel under pulsatile velocity inlet. On eccentric placement of single and two cylinders, FFT spectral analysis reveals a possible occurrence of *"lock-on"* phenomenon for the case of two cylinders placement at the gap ratio (B/H) of 5, which results in 8% increase in heat transfer as compared to the case of single cylinder of same aspect ratio at centric position. Moving the cylinder to the walls of the channel has a deteriorating effect on the heat transfer over the cylinder. It is expected that varying the amplitude or frequency of flow (at low Re) or the distance between the channel walls could substantially improve the heat transfer over the cylinder(s) of high aspect ratio, which the authors wish to carry out in the future work of this study.

References

[1] Zovatto, L., and Pedrizzetti, G., "Flow about a circular cylinder between parallel walls," *Journal of Fluid Mechanics*, vol. 440, 2001, pp. 1–25.

[2] Griffin, O., "Vortex shedding from bodies in a Shear Flow : A Review," *Journal of Fluids Engineering*, vol. 107, 1985, pp. 298–306.

[3] King, R., "A review of vortex shedding research and its application," *Ocean Engineering*, vol. 4, 1977, pp. 141–171.

[4] Roshko, A., "On the development of turbulent wakes from vortex streets," *National Advisory Committee for Aeronautics*, vol. Report 119, 1952, pp. 1–26.

[5] Monkewitz, P., "The absolute and convective nature of instability in 2-D wakes at low Reynolds numbers," *Phys. Fluids*, vol. 31, 1988, pp. 999–1006.

[6] Griffin, O., "Flow similitude and vortex lock-on in bluff body near wakes," *Phys. Fluids*, vol. A1, 1989, pp. 697–703.

[7] Hammache, M., and Gharib, M., "A novel methos to proote parallel vortex shedding in the wake of circular cylinders," *Phys. Fluids*, vol. A1, 1989, pp. 1611–1614.

[8] Prasad, A., and Williamson, C. H. K., "The instability of the shear layer separating from a bluff body," *Journal of Fluid Mechanics*, vol. 333, 1997, pp. 375–402.

[9] Arumuga Perumal, D., Kumar, G. V. S., and Dass, A. K., "Lattice Boltzmann simulation of flow over a circular cylinder at moderate reynolds numbers," *Thermal Science*, vol. 18, 2014, pp. 1235–1246.

[10] Kojouharova, J., and Weisweiler, H., "Modelling of fully separated flow past a circular cylinder: Problems and best practice," *Application of Mathematics in Technical and Natural Sciences*, vol. 70003, 2015, pp. 1–7.

[11] Niemann, H. J., and Hölscher, N., "A review of recent experiments on the flow past circular cylinders," *Journal of Wind Engineering and Industrial Aerodynamics*, vol. 33, 1990, pp. 197–209.

[12] Beaudan, P., and Moin, P., *Numerical Experiments on The Flow Past a Circular Cylinder at Sub-critical Reynolds Number*, 1994.

[13] Bijjam, S., and Dhiman, A. K., "CFD Analysis of Two-Dimensional Non-Newtonian Power-Law Flow Across a Circular Cylinder Confined in a Channel," *Chemical Engineering Communications*, vol. 199, 2012, pp. 767–785.

[14] Jiang, R. J., "Flow-induced vibrations of two tandem cylinders in a channel," *Thermal Science*, vol. 16, 2012, pp. 1377–1381.

[15] Jiang, R. J., Lin, J. Z., and Ku, X. K., "Flow-induced vibrations of two tandem circular cylinders in a parallel-wall channel," *Physics of Fluids*, vol. 26, 2014, pp. 1–22.

[16] Supradeepan, K., and Roy, A., "Characterisation and analysis of flow over two side by side cylinders for different gaps

at low reynolds number: A numerical approach," *Physics of Fluids*, vol. 26, 2014, pp. 1–29.

[17] Zdravkovich, M. M., *Flow Around Circular Cylinders: A Comprehensive Guide Through Flow Phenomena, Experiments, Applications, Mathematical Models, and Computer Simulations*, 2003.

[18] Jue, Horng-Wen Wu, Sheng-Yuan Huang, T.-C., "Heat Transferpredictions Around Three Heated Cylinders Between Two Parallel Plates," *Numerical Heat Transfer, Part A: Applications*, vol. 40, 2001, pp. 715–733.

[19] Galletti, B., Bruneau, C. H., Zannetti, L., and Iollo, A., "Low-order modelling of laminar flow regimes past a confined square cylinder," *Journal of Fluid Mechanics*, vol. 503, 2004, pp. 161–170.

[20] Perumal, D. A., Kumar, G. V. S., and Dass, A. K., "Numerical Simulation of Viscous Flow over a Square Cylinder Using Lattice Boltzmann Method," *ISRN Mathematical Physics*, vol. 2012, 2012, pp. 1–16.

[21] Saha, A., Biswas, G., and Muralidhar, K., "Three-dimensional study of flow past a square cylinder at low Reynolds numbers," *International Journal of Heat and Fluid …*, vol. 24, 2003, pp. 54–66.

[22] Dhiman, A. K., Chhabra, R. P., and Eswaran, V., "Flow and heat transfer across a confined square cylinder in the steady flow regime: Effect of Peclet number," *International Journal of Heat and Mass Transfer*, vol. 48, 2005, pp. 4598–4614.

[23] Sahu, A. K., Chhabra, R. P., and Eswaran, V., "Effects of Reynolds and Prandtl numbers on heat transfer from a square cylinder in the unsteady flow regime," *International Journal of Heat and Mass Transfer*, vol. 52, 2009, pp. 839–850.

[24] Sahu, A. K., Chhabra, R. P., and Eswaran, V., "Effects of Reynolds and Prandtl numbers on heat transfer from a square cylinder in the steady flow regime," *International Journal of Heat and Mass Transfer*, vol. 52, 2006, pp. 839–850.

[25] Bayraktar, S., Yayla, S., Oztekin, A., and Ma, H., "Wall proximity effects on flow over cylinders with different cross sections," *Can. J. Phys.*, vol. 92, 2014, pp. 1141–1148.

[26] Sau, A., Hsu, T. W., and Ou, S. H., "Three-dimensional evolution of vortical structures and associated flow bifurcations in the wake of two side-by-side square cylinders," *Physics of Fluids*, vol. 19, 2007, pp. 1–18.

[27] Knisely, C. W., "Strouhal numbers of rectangular cylinders at incidence: A review and new data," *Journal of Fluids and Structures*, vol. 4, 1990, pp. 371–393.

[28] Agelin-Chaab, M., and Tachie, M. F., "Open Channel Turbulent Flow past Rectangular Cylinders at Incidence," *Journal of Hydraulic Engineering*, vol. 139, 2013, pp. 1309–1313.

[29] Choi, C. B., and Yang, K. S., "Three-dimensional instability in flow past a rectangular cylinder ranging from a normal flat plate to a square cylinder," *Physics of Fluids*, vol. 26, 2014, pp. 1–8.

[30] Norberg, C., "Flow around rectangular cylinders: Pressure forces and wake frequencies," *Journal of Wind Engineering and Industrial Aerodynamics*, vol. 49, 1993, pp. 187–196.

[31] Yang, S.-J., and Fu, W.-S., "Numerical investigation of heat transfer from a heated oscillating rectangualr cylinder in a cross flow," *Numerical Heat Transfer, Part A*, vol. 39, 2001, pp. 569–591.

[32] Toppaladoddi, S., Dixit, H. N., Tatavarti, R., and Govindarajan, R., "Vortex shedding patterns, their competition, and chaos in flow past inline oscillating rectangular cylinders," *Physics of Fluids*, vol. 23, 2011, pp. 1–10.

[33] Lee, B.-S., Kim, T.-Y., and Lee, D.-H., "Control of Vortex Shedding Behind a Rectangular Cylinder Near the Ground," *Numerical Heat Transfer, Part A: Applications*, vol. 47, 2005, pp. 787–804.

[34] Kumaran, M., and Vengadesan, S., "Flow Characteristics Behind Rectangular Cylinder Placed Near a Wall," *Numerical Heat Transfer, Part A: Applications*, vol. 52, 2007, pp. 643–660.

[35] Sung, H. J., Hwang, K. S., and Hyun, J. M., "Experimental study on mass transfer from a circular cylinder in pulsating flow," *International Journal of Heat and Mass Transfer*, vol. 37, 1994, pp. 2203–2210.

[36] Barbi, C., Favier, D. P., Maresca, C. A., and Telionis, D. P., "Vortex shedding and lock-on of a circular cylinder in oscillatory flow," *J. Fluid Mech.*, vol. 170, 1986, pp. 527–544.

[37] Andraka, C. E., and Diller, T. E., "Heat-Transfer Distribution Around a Cylinder in Pulsating Crossflow," *Journal of Engineering for Gas Turbines and Power*, vol. 107, 1985, pp. 976–982.

[38] Gundappa, M., and Diller, T. E., "The effects of free-stream turbulence and flow pulsation on heat transfer from a cylinder in crossflow," *Journal of Heat Transfer (Transactions of the ASME (American Society of Mechanical Engineers)*, vol. 113, 1991, pp. 766–769.

[39] Iwai, H., Mambo, T., Yamamoto, N., and Suzuki, K., "Laminar convective heat transfer from a circular cylinder exposed to a low frequency zero-mean velocity oscillating flow," *International Journal of Heat and Mass Transfer*, vol. 47, 2004, pp. 4659–4672.

[40] Ji, T. H., Kim, S. Y., and Hyun, J. M., "Experiments on heat transfer enhancement from a heated square cylinder in a pulsating channel flow," *International Journal of Heat and Mass Transfer*, vol. 51, 2008, pp. 1130–1138.

[41] Yu, J.-Y., Lin, W., and Zheng, X.-T., "Effect on the flow and heat transfer characteristics for sinusoidal pulsating laminar flow in a heated square cylinder," *Heat and Mass Transfer*, vol. 50, 2014, pp. 849–864.

[42] Sharma, A., and Eswaran, V., "Heat and Fluid Flow Across a Square Cylinder in the Two-Dimensional Laminar Flow Regime," *Numerical Heat Transfer, Part A: Applications*, vol. 45, 2004, pp. 247–269.

[43] Blackburn, H. M., and Henderson, R. D., "A study of two-dimensional flow past an oscillating cylinder," *Journal of Fluid Mechanics*, vol. 385, 1999, pp. 255–286.

[44] Bourguet, R., Karniadakis, G. E., and Triantafyllou, M. S., "Multi-frequency vortex-induced vibrations of a long tensioned beam in linear and exponential shear flows," *Journal of Fluids and Structures*, vol. 41, 2013, pp. 33–42.

[45] Kiya, M., Mochizuki, O., Ishikawa, H., Gordnier, R. E., and Visbal, M. R., "Initial pressure distribution due to jet impact on a rigid body," *Journal of Fluids and Structures*, vol. 16, 2001, pp. 399–413.

[46] Mittal, S., and Tezduyar, T. E., "A Finite Element Study of Incompressible Flows Past Oscillating Cylinders and

Aerofoils," *Intl. J. for Numerical methods in fluids*, vol. 15, 1992, pp. 1073–1118.

[47] Ongoren, A., and Rockwell, D., "Flow structure from an oscillating cylinder Part 1. Mechanisms of phase shift and recovery in the near wake," *Journal of Fluid Mechanics*, vol. 191, 1987, pp. 197–223.

[48] Stansby, P. K., "The locking-on of vortex shedding due to the cross-stream vibration of circular cylinders in uniform and shear flows," *Journal of Fluid Mechanics*, vol. 74, 1976, pp. 641–665.

[49] Tanida, Y., Okajima, A., and Watanabe, Y., "Stability of a circular cylinder oscillating in uniform flow or in a wake," *Journal of Fluid Mechanics*, vol. 61, 1973, pp. 769–784.

[50] Okajima, A., "Strouhal numbers of rectangular cylinders," *Journal of Fluid Mechanics*, vol. 123, 1982, pp. 379–398.

[51] Biswas, G. Breuer, M., Durst, F. (Lehrstuhl fu¨r S., 4, U. E.-N. C., D-91058 Erlangen, G., and Breuer@lstm.uni-erlangen.de), "Backward-Facing Step Flows for Various Expansion Ratios at Low and Moderate Reynolds Numbers," *Journal of Fluids Engineering*, vol. 126, 2004, pp. 362–374.

[52] Stüer, H., Gyr, A., and Kinzelbach, W., "Laminar separation on a forward facing step," *European Journal of Mechanics - B/Fluids*, vol. 18, 1999, pp. 675–692.

[53] Velazquez, A., Arias, J. R., and Mendez, B., "Laminar heat transfer enhancement downstream of a backward facing step by using a pulsating flow," *International Journal of Heat and Mass Transfer*, vol. 51, 2008, pp. 2075–2089.

Ashish Saxena

Mr. Ashish Saxena is a full time Ph.D. student at Nanyang Technological University, Singapore. He is currently working on human skin temperature mapping for blood vessel blockage diagnosis. He has completed his Master's in Thermal Engineering from Birla Institute of Technology and Science-Pilani, Hyderabad Campus, India in 2015. His research interests include CFD and heat transfer, Thermo-regulation of solar photovoltaics, Nanofluids, and Biomedical diagnostic research.

Ng Yin Kwee, Eddie

Ng obtained a Ph.D at Cambridge University. He is the Editor-in-Chief for the ISI Journal of Mechanics in Medicine and Biology and the founding Editor-in-Chief for the ISI indexed Journal of Medical Imaging and Health Informatics. His main area of research is human physiology, biomedical engineering, computational fluid dynamics and numerical heat transfer.

1